Time-Dependent Flow seen through Approximate Observer Killing Fields

Markus Hadwiger, Matej Mlejnek, Thomas Theußl, and Peter Rautek

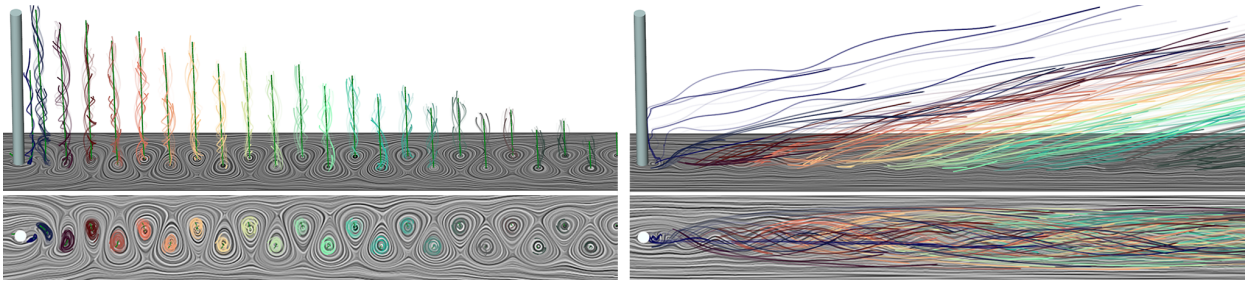

Fig. 1. **Observer field-relative visualization.** 2D von Kármán vortex street behind a circular cylinder. (Top) Space-time views with vertical time axes. (Bottom) Spatial domain. (Left) A *continuous observer field* follows the motion of the input flow by minimizing the *observed time derivative*. *Observed path lines* swirl around "vertical" vortex cores computed in the observed field, while LIC images depict *observed stream lines*. The observer field *jointly* perceives all vortices as stationary. Prior objective vortex detection methods would show the core lines in motion. (Right) The original lab frame observer perceives vortices and path lines as moving rightward.

Abstract—Flow fields are usually visualized relative to a global observer, i.e., a single frame of reference. However, often no global frame can depict all flow features equally well. Likewise, objective criteria for detecting features such as vortices often use either a global reference frame, or compute a separate frame for each point in space and time. We propose the first general framework that enables choosing a smooth trade-off between these two extremes. Using global optimization to minimize specific differential geometric properties, we compute a time-dependent observer velocity field that describes the motion of a continuous field of observers adapted to the input flow. This requires developing the novel notion of an observed time derivative. While individual observers are restricted to rigid motions, overall we compute an approximate Killing field, corresponding to almost-rigid motion. This enables continuous transitions between different observers. Instead of focusing only on flow features, we furthermore develop a novel general notion of visualizing how all observers jointly perceive the input field. This in fact requires introducing the concept of an observation time, with respect to which a visualization is computed. We develop the corresponding notions of observed stream, path, streak, and time lines. For efficiency, these characteristic curves can be computed using standard approaches, by first transforming the input field accordingly. Finally, we prove that the input flow perceived by the observer field is objective. This makes derived flow features, such as vortices, objective as well.

Index Terms—Flow visualization, observer frames of reference, Killing vector fields, infinitesimal isometries, Lie derivatives, objectivity

1 Introduction

A basic but fundamental challenge in flow visualization is that the perception of motion is always relative to some observer, even when this fact is not made explicit. This is not only true in special or general relativity. In Euclidean space, motion can also only be described relative to some chosen observer. This is known as *Galilean relativity* [2].

An important consequence of this fact is that basic concepts, such as flow being steady (time-independent) or unsteady (time-dependent), only have meaning with respect to a given and often only implied observer. That is, if a flow is steady for some observer $\mathbb{O}_0$, another observer $\mathbb{O}_1$ in relative motion will often perceive an unsteady flow.

However, these properties are of crucial importance for, e.g., the visualization of characteristic curves such as stream lines, or for line integral convolution [11]. Moreover, for features such as vortices, different feature detectors are *invariant* with respect to different classes of time-dependent transformations, e.g., Galilean invariance [10, 26], or rotation invariance [18]. More generally, frame-indifference or objectivity [46] commonly refers to invariance under rigid observer motion, and is considered a very desirable property of vortex detectors [17, 19–21].

Given the dependence of the perception of (particle) motion on observer motion, we present a general framework for describing the relative motion of flow and multiple observers. Instead of being limited to individual observers, we introduce a *continuous field* of observers, relative to which an arbitrary input flow field can be analyzed and visualized. Each observer in this field corresponds to its own individual reference frame that undergoes a time-dependent rigid motion. However, instead of considering different observers separately, we represent all of them by a single time-dependent *observer velocity field* $\mathbf{u}(x,t)$ that simultaneously describes the motion of the entire observer field.

Previous work usually either used one global frame, such as a frame spinning with the average vorticity of the domain [21], or, on the other end of the spectrum, computed frames adapted to local neighborhoods only [17, 50]. In contrast, our concept of an observer velocity field allows combining a global optimization with local adaptivity. A single optimization parameter allows for a smooth trade-off between the two.

We define an observer in Euclidean space to be limited to *rigid motions*, i.e., translations and rotations, which are the *isometries* of Euclidean space. However, for our framework we want to consider the description of an observer by a whole vector field. A vector field that corresponds to *infinitesimal isometries* is called a *Killing vector field* [37, Ch. 8], or simply a Killing field, named after Wilhelm Killing.

Given an arbitrary input flow field $\mathbf{v}(x,t)$, we can compute the observer field $\mathbf{u}(x,t)$ as a Killing field, while trying to "follow" the input

- *Markus Hadwiger, Matej Mlejnek, and Peter Rautek are with King Abdullah University of Science and Technology (KAUST), Visual Computing Center, Thuwal, 23955-6900, Saudi Arabia. E-mail: {markus.hadwiger, matej.mlejnek, peter.rautek}@kaust.edu.sa.*
- *Thomas Theußl is with King Abdullah University of Science and Technology (KAUST), Core Labs, Thuwal, 23955-6900, Saudi Arabia. E-mail: thomas.theussl@kaust.edu.sa.*

Manuscript received 31 Mar. 2018; accepted 1 Aug. 2018. Date of publication 16 Aug. 2018; date of current version 21 Oct. 2018. For information on obtaining reprints of this article, please send e-mail to: reprints@ieee.org, and reference the Digital Object Identifier below. Digital Object Identifier no. 10.1109/TVCG.2018.2864839

flow. We define *following the input flow* as observing the field $\mathbf{v}$ from an observer field $\mathbf{u}$ that perceives $\mathbf{v}$ to be *as steady as possible* [17, 31].

Outline and contributions. To follow realistic flow fields well, one observer and its rigid motion are usually not flexible enough [17, 19]. We approach this problem in the context of observer Killing fields by computing the observer field $\mathbf{u}$ as an *approximate* Killing field instead of an exact Killing field. This approach still allows each observer by itself to follow an exactly rigid motion, but in this way we allow *different points* in space to correspond to *different observers*. Nearby observers in general only *approximately* follow similar rigid motions.

"As steady as possible" flow means that all observers should perceive almost vanishing time derivatives. However, for this to be meaningful with respect to a general observer field $\mathbf{u}$, we have to define a suitably generalized concept of an observer-relative time derivative of the input field $\mathbf{v}$ with respect to $\mathbf{u}$. We call this the *observed time derivative* that we construct by building on the general concept of the *Lie derivative* from differential geometry [16, 29, 32]. We compute an observer field $\mathbf{u}$ that minimizes this observed time derivative via global optimization.

An *approximate observer Killing field* $\mathbf{u}$ enables several applications of general importance in flow visualization and continuum mechanics.

(1) We introduce generalizations of the standard stream lines, path lines, streak lines, and time lines to *observed* characteristic curves relative to an observer field $\mathbf{u}$, which enables visualizing what all observers *jointly* perceive. This requires introducing the concept of an *observation time*, with respect to which a visualization relative to the observer field is computed, because at another time the observers themselves will have moved and therefore an observer-relative visualization will be different. We note that while we mainly target approximate Killing fields, these generalizations in fact work for any general observer field.

(2) We apply the observer velocity field to the objective computation of vortices. This is enabled by the fact that our optimization is *guaranteed* to find the same unique observed field for any given input flow, for a chosen optimization parameter. We prove that this implies objectivity of the observed field, and thus of all properties derived from it.

Methodology. To be able to formulate our framework for a continuous field of observers, we employ methodology from differential geometry that is not commonly used in the flow visualization literature. We have already mentioned the concept of Killing fields [37] and approximate Killing fields [6, 28]. See App. C (suppl. material). The second crucial concept is the *Lie derivative* of a tensor field with respect to the flow of a vector field. In most differential geometry textbooks, e.g., [16, 29], the Lie derivative is only defined for time-independent flows, also called the autonomous Lie derivative [32, p.96]. Our framework, however, requires the less common Lie derivative for time-dependent flows, which is explained and used extensively by Marsden and Hughes [32, p.95]. We summarize the basics in Appendix A.

Notation. The domain where a vector field is defined is a manifold M, where in this paper $M = \mathbb{R}^2$ or $\mathbb{R}^3$. We denote the tangent space to M at a point $x \in M$ by $T_x M$. We extensively use the concept of the *flow* induced by a vector field [29]. See App. B (suppl. material). In particular, we denote a *time-dependent flow* by $\psi_{t,s}(x)$, following the notation of Marsden and Hughes [32], which maps the point x at time s to the corresponding point at time t, by integrating the underlying vector field along the path line through x from time s to time t. We note that in flow visualization, $\psi_{t,s}$ is often written as a *flow map* ϕ_t^τ, sometimes with the meaning $\psi_{t+\tau,t}$ instead of $\psi_{\tau,t}$, which changes the meaning of $(\partial/\partial s)\,\psi_{t,s}$, and, unlike our notation, does not have $\psi_{t,s}^{-1} = \psi_{s,t}$.

For maps, we often use explicit notation to denote which arguments are variable, e.g., instead of $\psi_{t,s}(x)$ we can write $t \mapsto \psi_{t,s}(x)$ with s and x fixed, which defines a path line. Using the same flow $\psi_{t,s}(x)$, a streak line is then given by $s \mapsto \psi_{t,s}(x)$ with t and x fixed instead.

We denote the *differential* of $\psi_{t,s}$ by $\mathrm{d}\psi_{t,s}$, also called the tangent map, or the (pointwise) *push-forward* [29]. This is the standard concept on manifolds in differential geometry, where the push-forward of a map $\psi_{t,s}$ is often written as $\psi_{t,s*}$. The differential is a linear map between tangent spaces. See App. B (suppl. material). In flow visualization, this map is often written as the "spatial gradient" $\nabla\phi_t^\tau$ of the flow map ϕ_t^τ.

Finally, we denote the time-dependent Lie derivative by $L_{\mathbf{u}}$, and the autonomous Lie derivative by $\mathscr{L}_{\mathbf{u}}$. See the summary in Appendix A.

2 Related Work

Flow visualization implicitly depends on an observer. This is often the lab frame observer with respect to which a vector field is initially given (computed or measured). We denote this observer by $\mathbb{O}_0$. This is crucial for considering flow as steady or unsteady, which affects all basic characteristic (integral) curves [5], such as stream, path, streak, and time lines. Many basic techniques, such as LIC [11], have been defined only for steady flow, although variants for unsteady flow exist, e.g., UFLIC [30, 41]. Texture advection techniques [27, 47] specifically consider unsteady flow. The important point for us is that whether a flow is perceived as being steady or unsteady is observer-dependent.

Euclidean observers. The concept of an observer in Euclidean space has been recognized to be of importance in fluid mechanics [20] as well as in flow visualization [17]. A standard reference in continuum mechanics is Truesdell and Noll [46], who define a transformation between two observers that is often used [17, 20–22, 35]. Holzapfel [22] and Ogden [35] have more detailed and approachable explanations.

The concept of *objectivity* (frame-indifference) has been introduced with respect to this observer transformation. See Truesdell [46, p.41], Holzapfel [22, Ch. 5], and Ogden [35, Ch. 2.1]. Most methods that explicitly consider observers treat only a *global* observer, in the sense that the observer transformation is considered to be the same everywhere.

Multiple observers. While not originally presented as such, the Galilean-invariant vortex detection method of Weinkauf et al. [50] computes a different constant-velocity observer at each point in time and space. Each observer is computed separately, and their method is not objective. The objective method of Günther et al. [17] computes a different rigid-motion observer for each point in time and space via optimization. However, each observer is computed separately, individually optimizing over a relatively large, constant-size neighborhood (see also Sec. 9). Bujack et al. [10] consider multiple observers via a weighted average of vector fields seen from a finite number of certain Galilean-invariant critical points. They compute a *joint* visualization for all observers, which we also do (see also App. H, suppl. m.). Their method is 2D only, treats each time step individually, and is not objective.

Flow decomposition methods, such as variants of the Helmholtz-Hodge decomposition [7, 8], can also be used to remove background flow, corresponding to the harmonic component [9]. These methods treat each time step individually, without considering time derivatives.

Vortex detection. Vortex dynamics are an important topic in fluid mechanics [39], with many different criteria available for vortex detection [19]. Many methods were originally defined for steady flow, such as the method of Sujudi and Haimes [44], but some have been extended to unsteady flow [50]. Galilean invariance of these critera is considered to be important [19]. Other kinds of invariance have been defined as well, such as the specific kind of rotation invariance of Günther et al. [18]. The more general property of objectivity [20, 46] is often achieved by defining new, objective vortex criteria [20]. Some criteria can be seen as being relative to a specific global observer, such as the LAVD criterion of Haller et al. [21] that becomes objective relative to the average vorticity of the domain, which is equivalent to an observer spinning with this vorticity. The approach of Günther et al. [17] computes an objective velocity field and its derivatives, and therefore makes all criteria computed from these properties automatically objective.

Killing fields are special vector fields whose induced flow preserves distances, i.e., they are infinitesimal isometries. In Euclidean space, they correspond to (the derivatives of) all rigid motions, which is crucial to our approach. Basics of rigid motions and Killing fields are discussed by Kilian et al. [28] and Ben-Chen et al. [6]. Details are described by McInerney [34, p.249]. More advanced presentations are given by Petersen [37], and do Carmo [15]. Approximate Killing fields have been used in shape deformation [33], shape space exploration [28], planar as-Killing-as-possible vector fields [43], on curved surfaces [6], and for designing approximate Killing fields on meshes [3, 4]. Approximate Killing fields have also been used for the decomposition of 2-tensors in a compact region of 2D Euclidean space [14], and for non-rigid image registration [13]. As-rigid-as-possible approaches for shape interpolation [1], or shape manipulation [23], are also similar, although they use finite (integrated) rotations instead of infinitesimal isometries.

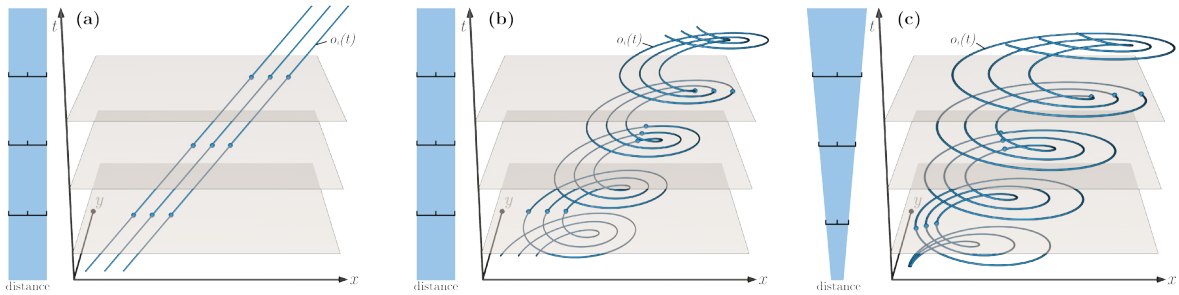

Fig. 2. **Observer velocity fields and observer world lines.** Observer velocity fields describe the motions of a continuous field of observers $\mathbb{O}_i$, with $i \in M$, relative to some observer $\mathbb{O}_0$. We depict the *world lines* $t \mapsto o_i(t)$ of three observers in three observer fields $\mathbf{u}$. In (a) and (b), all world lines in fact correspond to different points of *the same* observer, since they follow the same global rigid motion. These observer fields are *exact* Killing fields. The observer field in (c) exhibits world lines of observers not following the same rigid motion, and thus can only be an *approximate* Killing field.

3 Vector Fields Describing Rigid Motions

We describe the motion of an observer $\mathbb{O}_1$ as a *Killing field* $\mathbf{u}_1(x,t)$, which must be interpreted relative to some other observer $\mathbb{O}_0$. In Euclidean space, the requirement that $\mathbf{u}_1(x,t)$ must be a Killing field corresponds to the fact that an observer can only undergo rigid motion.

3.1 Rigid body motion

The motion described by a time-dependent vector field $(x,t) \mapsto \mathbf{u}(x,t)$ describes a rigid motion if and only if it can be written as (see [28])

$$\mathbf{u}(x,t) = \mathbf{w}(t) + \mathbf{\Omega}(t)(x-o), \tag{1}$$

where $\mathbf{u}$ is a vector field, $\mathbf{w}$ is a time-dependent vector-valued function, and x and o are points in space. The skew-symmetric tensor $\mathbf{\Omega}(t)$ is the spin (vorticity) tensor at time t, corresponding to an infinitesimal rotation, like the corresponding angular velocity pseudovector $\boldsymbol{\omega}(t)$ [25]. While x and t are variables, o is a fixed, but arbitrary, point in space. Using a fixed point o corresponds to an *Eulerian* viewpoint (see below).

Corresponding to all rigid motions, in Euclidean space a vector field $\mathbf{u}(x,t)$ is a Killing field iff it can be written in the form of Eq. 1.

3.2 Relative observer motion

Now, instead of considering the motion of a rigid body with respect to an observer $\mathbb{O}_0$, we consider the rigid motion of *another observer* $\mathbb{O}_1$, again relative to the observer $\mathbb{O}_0$. While at each fixed time t, the point o must be fixed in Eq. 1, it is not necessary that o is the same point at different times. This corresponds to whether we choose to use an *Eulerian* or a *Lagrangian* perspective. We therefore rewrite Eq. 1 as

$$\mathbf{u}_1(x,t) = \mathbf{w}(t) + \mathbf{\Omega}(t)(x-o(t)), \tag{2}$$

where now $t \mapsto o(t)$ gives a fixed point in space for each time t, but $o(t)$ can vary over time. We require that $t \mapsto o(t)$ is a smooth function of t, which describes the curve that the point o traces out in space over time.

Eulerian viewpoint (relative to $\mathbb{O}_0$). We can *choose* $t \mapsto o(t)$ to describe some point o_0 that the observer $\mathbb{O}_0$ perceives as *stationary*, i.e., as undergoing no relative motion. In general, however, the point o_0 is moving relative to $\mathbb{O}_1$. That is, $\mathbb{O}_1$ sees $t \mapsto o(t) = o_0$ tracing out a curve, whereas for $\mathbb{O}_0$ it is a fixed point. If we set $o(t) = o_0$, considering $x = o_0$ shows that the $\mathbf{w}(t)$ in Eq. 2 has to be $\mathbf{w}(t) = \mathbf{u}_1(o_0,t)$. Thus,

$$\mathbf{u}_1(x,t) = \mathbf{u}_1(o_0,t) + \mathbf{\Omega}(t)(x-o_0), \tag{3}$$

where the function $t \mapsto \mathbf{w}(t) = \mathbf{u}_1(o_0,t)$ describes the *Eulerian velocity* of observer $\mathbb{O}_1$, observed at the point o_0 fixed relative to observer $\mathbb{O}_0$. However, observer $\mathbb{O}_1$ will see this o_0 as *different* points over time.

Lagrangian viewpoint (relative to $\mathbb{O}_0$). We can instead choose $o(t)$ to describe the curve of a point that observer $\mathbb{O}_0$ perceives as *moving with* $\mathbb{O}_1$, while being stationary for observer $\mathbb{O}_1$. With this $o(t)$, the $\mathbf{w}(t)$ from Eq. 2 now becomes $\mathbf{w}(t) = \mathbf{u}_1(o_1(t),t)$, and we therefore get

$$\mathbf{u}_1(x,t) = \mathbf{u}_1(o_1(t),t) + \mathbf{\Omega}(t)(x-o_1(t)), \tag{4}$$

where now $t \mapsto \mathbf{w}(t) = \mathbf{u}_1(o_1(t),t)$ denotes the *Lagrangian velocity* of the point $o_1(t)$ undergoing the same motion as $\mathbb{O}_1$, as perceived by $\mathbb{O}_0$.

Relationship between viewpoints. It is a crucial fact that, while the Lagrangian and the Eulerian viewpoints assign a completely different meaning to the function $t \mapsto \mathbf{w}(t)$, the vector field $(x,t) \mapsto \mathbf{u}_1(x,t)$, given relative to the observer $\mathbb{O}_0$, is *identical* for both views, i.e., it is *independent of whether we use the Lagrangian or the Eulerian view.*

However, the Lagrangian viewpoint is what will enable us to model an entire *field* of observers $\mathbf{u}_i(x,t)$ by *one observer velocity field* $\mathbf{u}(x,t)$.

4 Observer Fields

Building on the relative motion between two observers $\mathbb{O}_0$ and $\mathbb{O}_1$, we now define a whole *field* of observers $\mathbb{O}_i$, again relative to the observer $\mathbb{O}_0$. See Fig. 2. We can (but need not) choose $\mathbb{O}_0$ as the "lab frame" where the input field $\mathbf{v}$ is given. However, it is crucial to note that while *some* choice of $\mathbb{O}_0$ is necessary to be able to specify relative motion, we can easily transform a representation relative to $\mathbb{O}_0$ to one relative to any other $\bar{\mathbb{O}}_0$. Both will represent the same observer field.

4.1 Sets of observers and observer world lines

Abstractly, we can define a set of observers $\mathbb{O}_i := \mathbb{O}(i)$, $i \in I$, by a map

$$\mathbb{O}\colon i \mapsto \Big(t \mapsto o_i(t), t \mapsto \mathbf{\Omega}_i(t)\Big). \tag{5}$$

This simply means that each observer is described by a pair of time-dependent functions $t \mapsto o_i(t)$ and $t \mapsto \mathbf{\Omega}_i(t)$, where $i \in I$ is an index from an index set I. We want to define a continuous set of observers, where each observer is adapted to a local neighborhood in space. We therefore choose the index set to be $I = M$. That is, we define an observer $\mathbb{O}_i$ for each position $x = i \in M$ on the manifold $M = \mathbb{R}^2$ or $\mathbb{R}^3$.

As in Sec. 3.2, the functions $t \mapsto o_i(t)$ are curves on M. We therefore choose a spatial indexing of the observers $\mathbb{O}_i$ by choosing $i = o_i(t_0)$, for some arbitrarily chosen time t_0. We furthermore require that, at any time t, all of M is "filled" by the positions $i \mapsto o_i(t)$ for fixed t, i.e.,

$$\bigcup_{i \in I} o_i(t) = M, \quad \text{for all fixed } t. \tag{6}$$

We can say that M is always filled by a *continuous field* of observers.

Observer world lines. We can say that *one fixed choice of point* of each observer $\mathbb{O}_i$ is located at $o_i(t)$ at time t, and each curve $t \mapsto o_i(t)$ describes how this point moves over time. Therefore, the curve $t \mapsto o_i(t)$ is the *world line* [2, p.8] of the point $o_i(t_0)$ of observer $\mathbb{O}_i$. We also say simply that it is the *world line of observer* $\mathbb{O}_i$. The world lines of all other points of observer $\mathbb{O}_i$ can easily be computed from Eq. 10 below.

4.2 The observer velocity field

Instead of storing the functions in Eq. 5 explicitly for each observer $\mathbb{O}_i$, we can represent them by a single smooth, time-dependent *observer velocity field* $(x,t) \mapsto \mathbf{u}(x,t)$. For all observers $\mathbb{O}_i$, we can simply *define* the functions $t \mapsto o_i(t)$ and $t \mapsto \mathbf{\Omega}_i(t)$ based on the vector field $\mathbf{u}$ as

$$t \mapsto o_i(t) := o_i(t_0) + \int_{t_0}^{t} \mathbf{u}(o_i(\tau),\tau)\, \mathrm{d}\tau, \tag{7}$$

$$t \mapsto \mathbf{\Omega}_i(t) := \frac{1}{2}\Big(\nabla\mathbf{u} - (\nabla\mathbf{u})^T\Big)(o_i(t),t), \tag{8}$$

where $\nabla\mathbf{u}$ denotes the (spatial) *velocity gradient tensor* of $\mathbf{u}$. In this way, the observer field will be smooth in space and time (for smooth $\mathbf{u}$), and the observers whose world lines $o_i(t)$ are spatially close in some time interval $t \pm \delta t$ will undergo similar motions and have similar spin in $t \pm \delta t$. Over time, these observers can start to differ more and more, but since the observer field is continuous, at any point in time there will always be "nearby" observers whose motion is similar. We can say

- Each world line $t \mapsto o_i(t)$ is a smooth curve describing the Lagrangian motion of (one chosen point of) observer $\mathbb{O}_i$. Nearby observers undergo similar motions (in a time interval $t \pm \delta t$).
- Each $t \mapsto \mathbf{\Omega}_i(t)$ is a smooth curve through $\mathfrak{so}(n)$ (with $n = 2$ or 3), the Lie algebra of infinitesimal rotations, describing observer spin. The corresponding Lie group $SO(n)$ represents finite rotations. Nearby observers will have similar spin (in a time interval $t \pm \delta t$).

Given the above, from all world lines $t \mapsto o_i(t)$ we of course have

$$t \mapsto \mathbf{u}\left(o_i(t),t\right) = \frac{\mathrm{d}}{\mathrm{d}\tau}\bigg|_{\tau=t} o_i(\tau), \tag{9}$$

and therefore, due to the existence and uniqueness theorem of ordinary differential equations, the curves $t \mapsto o_i(t)$ are well-defined by the vector field $\mathbf{u}$, and they never intersect in space-time. This gives Eq. 6.

Approximate Killing field for all observers. In order to obtain the flexibility to adapt the described observer motion to any input flow field $\mathbf{v}(x,t)$, we can compute (Sec. 5) the observer velocity field $\mathbf{u}(x,t)$ to be an *approximate*, instead of an exact, Killing field. This allows nearby observers to be different, while still keeping them "as similar as possible." This approach essentially restricts the rate of deformation (cf. Eq. 24) of the observer field, compared to exact rigid motion.

Exact Killing fields for individual observers. Nevertheless, from the field $\mathbf{u}(x,t)$ we can still obtain the *exact* Killing field $\mathbf{u}_i(x,t)$ describing the rigid motion of any chosen observer $\mathbb{O}_i$. We simply use the Lagrangian viewpoint following the world line $t \mapsto o_i(t)$, and *define*

$$\mathbf{u}_i(x,t) := \mathbf{u}\left(o_i(t),t\right) + \mathbf{\Omega}_i(t)\left(x - o_i(t)\right), \tag{10}$$

where $\mathbf{u}(x,t)$ is the observer velocity field, and $\mathbf{u}_i(x,t)$ describes the rigid motion of $\mathbb{O}_i$. The crucial observation that makes this construction possible is that all the velocity fields $\mathbf{u}_i(x,t)$ are completely independent of the choice of the points $o_i(t_0)$. We can therefore easily fulfill Eq. 6.

Killing property of each $\mathbf{u}_i$. We know that for all observers $\mathbb{O}_i$, the vector field $\mathbf{u}_i(x,t)$ given by Eq. 10 is a Killing field, since it describes the rigid motion (cf. Eq. 4) of observer $\mathbb{O}_i$. Correspondingly, for the (spatial) velocity gradient tensor of $x \mapsto \mathbf{u}_i(x,t)$ with t fixed, we get

$$x \mapsto \nabla\mathbf{u}_i(x,t) = \mathbf{\Omega}_i(t), \quad \text{for every fixed } t. \tag{11}$$

We can also see this by noting that for any fixed t, the term $\mathbf{u}\left(o_i(t),t\right)$ is constant on M. After taking the spatial gradient, only the spin remains.

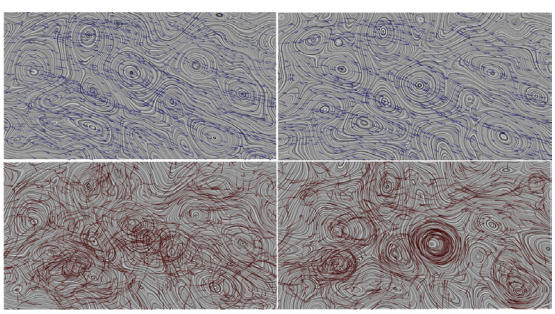

Fig. 3. **Observers following an unsteady flow field.** (Top) Two successive time steps of the OCEAN flow (LIC). The blue particles illustrate how the observer field $\mathbf{u}$ follows the input motion. (Bottom) Particles advected by the flow trace out path lines (brown). (Bottom left) For the observer $\mathbb{O}_0$, they are hard to interpret. (Bottom right) From the perspective of the observer field $\mathbf{u}$, path lines are much more steady because the observers follow the flow, and the observed time derivative $\mathscr{D}/\mathscr{D}t(\mathbf{v_u})$ is small.

4.3 Observer-relative velocities and time derivatives

Given an observer velocity field $\mathbf{u}(x,t)$, which does not have to be an exact Killing field, we want to consider *observer-relative* Eulerian time derivatives of an arbitrary input field $\mathbf{v}(x,t)$, relative to the observers described by $\mathbf{u}$. These time derivatives are an important term in the optimization for computing $\mathbf{u}$ adapted to $\mathbf{v}$, as described in Sec. 5.

Observer-relative velocities. We first note that the velocity field describing how an arbitrary individual observer $\mathbb{O}_i$ perceives the instantaneous motion described by $\mathbf{v}$ is simply the relative velocity field

$$\mathbf{v}_{\mathbf{u}_i} := \mathbf{v} - \mathbf{u}_i. \tag{12}$$

The crucial point now is that a single expression for all observers perceiving $\mathbf{v}$ locally at any position $o_i(t)$, for any i and t, is simply

$$\mathbf{v}_\mathbf{u} = \mathbf{v} - \mathbf{u}, \tag{13}$$

since at each $o_i(t)$, $\mathbf{u}_i = \mathbf{u}$ (Eq. 10). The vector field $\mathbf{v}_\mathbf{u}$ is objective [46], because the non-objective part resulting from any observer transformation applied to both $\mathbf{v}$ and $\mathbf{u}$ cancels out. See App. F (suppl. material).

Observed time derivatives. We now want to obtain a meaningful observer-relative time derivative of $\mathbf{v}_\mathbf{u}$ as observed by $\mathbf{u}$. This requires a derivative of $\mathbf{v}_\mathbf{u}$ *with respect to the flow* of the field $\mathbf{u}$. The derivative of a time-dependent vector field $\mathbf{v}$ with respect to the flow of another vector field $\mathbf{u}$ is given by the time-dependent *Lie derivative* $L_\mathbf{u}\mathbf{v}$ (Eq. 53).

We thus define the *observed time derivative* of $\mathbf{v}_\mathbf{u}$ relative to $\mathbf{u}$ as

$$\frac{\mathscr{D}}{\mathscr{D}t}\mathbf{v}_\mathbf{u} := L_\mathbf{u}(\mathbf{v}_\mathbf{u}). \tag{14}$$

This derivative is, in fact, the time derivative of $\mathbf{v}$ relative to the motion and deformation of the field $\mathbf{u}$, and likewise the Eulerian time derivative in our observation time fields $\mathbf{w}_r$ (Sec. 6.3). See Fig. 4 (bottom row).

Computation. In order to compute Eq. 14, we again work relative to the observer $\mathbb{O}_0$, but again emphasize that this is an arbitrary choice. In fact, we note that Lie derivatives of objective tensors (here, $\mathbf{v}_\mathbf{u}$) are always objective, even though the vector field $\mathbf{u}$ is not [32, Th. 6.19]. From linearity [32, Prop. 6.14 (iii)], and from Eqs. 13 and 53, we get

$$\begin{aligned} L_\mathbf{u}(\mathbf{v}_\mathbf{u}) &= L_\mathbf{u}(\mathbf{v}-\mathbf{u}) = L_\mathbf{u}(\mathbf{v}) - L_\mathbf{u}(\mathbf{u}), \\ &= \left(\frac{\partial\mathbf{v}}{\partial t} + \mathscr{L}_\mathbf{u}\mathbf{v}\right) - \left(\frac{\partial\mathbf{u}}{\partial t} + \mathscr{L}_\mathbf{u}\mathbf{u}\right) = \frac{\partial\mathbf{v}_\mathbf{u}}{\partial t} + \mathscr{L}_\mathbf{u}\mathbf{v}, \end{aligned} \tag{15}$$

since the autonomous Lie derivative of a vector field with respect to itself, here the term $\mathscr{L}_\mathbf{u}\mathbf{u}$, is always zero [32, Prop. 6.14 (vii)]. Expanding the autonomous Lie derivative $\mathscr{L}_\mathbf{u}\mathbf{v}$ (Eq. 51) then gives

$$\frac{\mathscr{D}}{\mathscr{D}t}\mathbf{v}_\mathbf{u} = \frac{\partial\mathbf{v}}{\partial t} - \frac{\partial\mathbf{u}}{\partial t} + \nabla\mathbf{v}\left(\mathbf{u}\right) - \nabla\mathbf{u}\left(\mathbf{v}\right). \tag{16}$$

Using the optimization procedure described below, for any given input field $\mathbf{v}$, we compute the field $\mathbf{u}$ to minimize this expression. This gives us an *as steady as possible* observed field $\mathbf{v}_\mathbf{u}$. See Fig. 3 (bottom right).

Rigid observer motion. We can also see that the Lie derivative $L_\mathbf{u}(\mathbf{v}_\mathbf{u})$ is the correct general concept by deriving $\mathscr{D}/\mathscr{D}t(\mathbf{v}_\mathbf{u})$ for rigid motion, i.e., for an exactly Killing $\mathbf{u}$ with $\nabla\mathbf{u} = \mathbf{\Omega}$. See App. D (suppl. material) for a derivation without Lie derivatives that agrees with Eq. 16.

Galilean observer motion. Further limiting general rigid observer motion to the Galilean case, i.e., constant translational motion, Eq. 16 of course also gives the correct result. That is, for observer motion with a constant velocity $\mathbf{u}$, we have $\frac{\partial\mathbf{u}}{\partial t} = 0$ and $\nabla\mathbf{u}(\mathbf{v}) = \mathbf{\Omega}\mathbf{v} = 0$ (no observer spin), and so Eq. 16 becomes the time derivative for the Galilean case,

$$\frac{\mathscr{D}}{\mathscr{D}t}\mathbf{v}_\mathbf{u} = \frac{\partial\mathbf{v}}{\partial t} + \nabla\mathbf{v}\left(\mathbf{u}\right). \tag{17}$$

4.4 Input flow perceived by an individual observer

From the above, we can now derive how an arbitrary *individual* observer $\mathbb{O}_i$ perceives the motion described by $\mathbf{v}$. These differential properties can be used together with standard flow feature detectors,

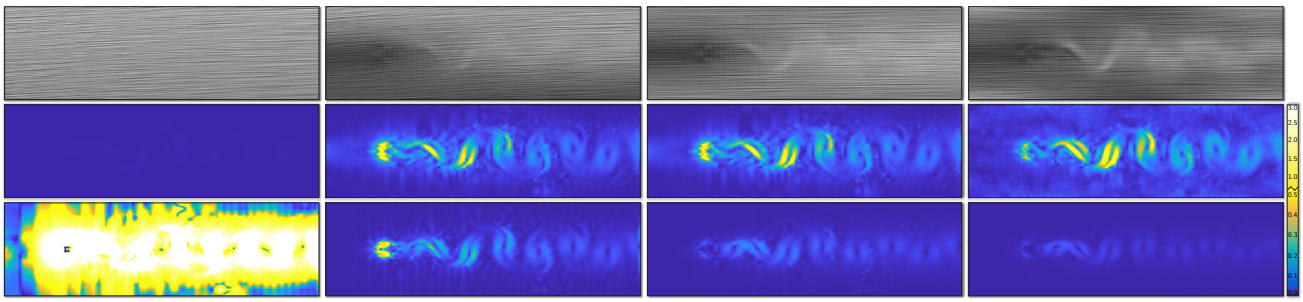

(a) λ=0.01 μ=0.01 (b) λ=1.0 μ=0.05 (c) λ=4.0 μ=0.05 (d) λ=12.0 μ=0.05

Fig. 4. **Optimizing observer fields** for the 2D VORTEX STREET with different parameters λ,μ in Eq. 25: (a) Killing $\mathbf{u}$ ($\lambda=0.01,\mu=0.01$); (b) Approximate Killing $\mathbf{u}$ ($\lambda=1.0,\mu=0.05$), as in Fig. 1; (c) Slightly higher Killing energy $\mathbf{u}$ ($\lambda=4.0,\mu=0.05$); (d) Higher energy $\mathbf{u}$ ($\lambda=12.0,\mu=0.05$). (Top row) LIC of each observer field $\mathbf{u}$ (shade: $\|\mathbf{u}\|_2$); (Middle row) Killing energy $\|K\mathbf{u}\|_F$; (Bottom row) Observed time derivative $\|\mathscr{D}/\mathscr{D}t\,\mathbf{v}_\mathbf{u}\|_2$.

such as standard vortex detectors. Analogously to Günther et al. [17], these measures then become objective. Relative to the rigid motion described by $\mathbf{u}_i$, the input vector field $\mathbf{v}$ and its derivatives become

$$\mathbf{v}_{\mathbf{u}_i} = \mathbf{v}-\mathbf{u}_i, \tag{18}$$

$$\nabla\mathbf{v}_{\mathbf{u}_i} = \nabla\mathbf{v}-\boldsymbol{\Omega}_i, \tag{19}$$

$$\frac{\mathscr{D}}{\mathscr{D}t}\mathbf{v}_{\mathbf{u}_i} = \frac{\partial\mathbf{v}}{\partial t}-\frac{\partial\mathbf{u}_i}{\partial t}+\nabla\mathbf{v}(\mathbf{u}_i)-\boldsymbol{\Omega}_i\mathbf{v}, \tag{20}$$

$$\mathbf{a}_{\mathbf{u}_i} = \mathbf{a}-\frac{\partial\mathbf{u}_i}{\partial t}-2\boldsymbol{\Omega}_i\mathbf{v}+\boldsymbol{\Omega}_i\mathbf{u}_i. \tag{21}$$

Eq. 18 is Eq. 12. Eq. 19 is the spatial gradient operator ∇ applied to Eq. 18, and, since $\mathbf{u}_i$ is Killing (Eq. 11), $\nabla\mathbf{u}_i=\boldsymbol{\Omega}_i$. Eq. 20 is Eq. 16 with $\nabla\mathbf{u}_i=\boldsymbol{\Omega}_i$. Eq. 21 is given by the observed material acceleration $\mathbf{a}_{\mathbf{u}_i}=\mathscr{D}/\mathscr{D}t(\mathbf{v}_{\mathbf{u}_i})+\nabla\mathbf{v}_{\mathbf{u}_i}(\mathbf{v}_{\mathbf{u}_i})$, the observed material time derivative of $\mathbf{v}_{\mathbf{u}_i}$.

Computation from u. At any $x=o_i(t)$, we can avoid computing the field $\mathbf{u}_i$ (Eq. 10) and $\partial\mathbf{u}_i/\partial t$, by computing everything from the field $\mathbf{u}$. At every point $o_i(t)$, we have $\mathbf{u}_i=\mathbf{u}$, and in order to obtain $\partial\mathbf{u}_i/\partial t$ directly from $\mathbf{u}$, computing the Eulerian time derivative of Eq. 10 gives

$$\left.\frac{\partial\mathbf{u}_i}{\partial t}\right|_{\substack{x=o_i(\tau)\\t=\tau}} = \frac{\partial\mathbf{u}}{\partial t}+\nabla\mathbf{u}(\mathbf{u})-\boldsymbol{\Omega}_i\mathbf{u} = \frac{\partial\mathbf{u}}{\partial t}+\frac{1}{2}\left(\nabla\mathbf{u}+(\nabla\mathbf{u})^T\right)\mathbf{u}, \tag{22}$$

where Eq. 8 was used to get $\boldsymbol{\Omega}_i$ from $\mathbf{u}$. From this and Eq. 16, we get

$$\left.\frac{\mathscr{D}}{\mathscr{D}t}\mathbf{v}_{\mathbf{u}_i}\right|_{\substack{x=o_i(\tau)\\t=\tau}} = \frac{\mathscr{D}}{\mathscr{D}t}\mathbf{v}_\mathbf{u}+\frac{1}{2}\left(\nabla\mathbf{u}+(\nabla\mathbf{u})^T\right)\mathbf{v}_\mathbf{u}. \tag{23}$$

This equation can be used to compute $\mathscr{D}/\mathscr{D}t\,\mathbf{v}_{\mathbf{u}_i}$ from $\mathbf{v}$, $\mathbf{u}$, and Eq. 16. Importantly, this also shows that by computing the observer velocity field $\mathbf{u}$ via optimization as given below, we in fact also minimize $\mathscr{D}/\mathscr{D}t\,\mathbf{v}_{\mathbf{u}_i}$, by explicitly minimizing all other terms in Eq. 23.

5 COMPUTING APPROXIMATE OBSERVER KILLING FIELDS

In order to compute an observer velocity field $\mathbf{u}(x,t)$ that is adapted to an arbitrary input field $\mathbf{v}(x,t)$, we define an energy functional that corresponds to desired characteristics of the observer field, and then compute $\mathbf{u}$ as the minimizer of this functional over all of M, and all time, using global optimization. We first formulate the desired individual criteria, and then formulate the corresponding minimization problem.

5.1 Desired criteria for observer velocity fields

We target a balance between the following three criteria for the computation of the observer velocity field $\mathbf{u}$, emphasizing the first two.

1. Observer fields should be (approximate) Killing fields. In order to obtain an approximate Killing field for the observer velocity field $\mathbf{u}$, the (spatial) velocity gradient tensor $\nabla\mathbf{u}$ of $x\mapsto\mathbf{u}(x,t)$ for each fixed t must be enforced to be anti-symmetric at all points $x\in M$ [37]. We thus define the *Killing operator* K [6, Def. 4], operating on $\mathbf{u}$ by

$$K\mathbf{u} := \nabla\mathbf{u}+(\nabla\mathbf{u})^T, \tag{24}$$

which is twice the symmetric part of the velocity gradient $\nabla\mathbf{u}$, i.e., twice the standard rate-of-strain tensor [46] of $\mathbf{u}$. The Killing operator measures, pointwise, the part of $\mathbf{u}$ that prevents it from being Killing. Minimizing this expression computes $\mathbf{u}$ as an *approximate* Killing field.

2. Follow the input field: minimize the observed time derivative. In order to make the observation of $\mathbf{v}$ *as steady as possible*, we want an observer field that results in a small observed time derivative $\mathscr{D}/\mathscr{D}t\,\mathbf{v}_\mathbf{u}$.

3. Regularization: match the input field. For regularization, we will match the input field as much as possible, i.e., we target small $\mathbf{v}_\mathbf{u}$.

Rationale for criteria. The first two criteria correspond to the main goals for an observer field stated in the introduction: (1) The field $\mathbf{u}$ should be "as Killing as possible," which makes nearby observers as similar as possible, and will give visualizations with as little deformation as possible. Mathematically, this means that the Killing energy should be as small as possible. (2) The observed field $\mathbf{v}_\mathbf{u}$ should have almost vanishing observed time derivative, i.e., be as steady as possible.

The third criterion above fulfills two purposes: (1) Choose a unique solution if there are (infinitely) many solutions with the same minimum. We choose the solution that is most similar to the input field, "following" it in this sense as well. (2) Corresponding to Eq. 23, it also helps enforce a minimal difference between the observed time derivative relative to exact rigid motion ($\mathbf{u}_i$) and that of only approximately rigid motion ($\mathbf{u}$).

5.2 Formulating the minimization problem

According to the three criteria given above, we formulate the following global optimization problem, over the space of all possible fields $\mathbf{u}$ in some function space $\mathscr{V}$ of vector fields (e.g., C^n vector fields) on M:

$$\min_{\mathbf{u}\in\mathscr{V}}\int_{\tau,\xi}\left(E_K+\lambda D_t+\mu R\right)(\mathbf{u},\xi,\tau)\,\mathrm{d}\xi\,\mathrm{d}\tau, \tag{25}$$

with relative weights $\lambda,\mu\in\mathbb{R}$. The individual terms are (see Fig. 4),

$$E_K(\mathbf{u},\xi,\tau) := \frac{1}{2}\|K\mathbf{u}(\xi,\tau)\|_F^2, \tag{26}$$

$$D_t(\mathbf{u},\xi,\tau) := \frac{1}{2}\left\|\frac{\mathscr{D}}{\mathscr{D}t}\mathbf{v}_\mathbf{u}(\xi,\tau)\right\|_2^2, \tag{27}$$

$$R(\mathbf{u},\xi,\tau) := \frac{1}{2}\|\mathbf{v}_\mathbf{u}(\xi,\tau)\|_2^2. \tag{28}$$

Integrating E_K over the domain gives the *Killing energy* of the observer field $\mathbf{u}$ [6, Def. 5]. $\|\cdot\|_F$ denotes the Frobenius norm, $\|\cdot\|_2$ the 2-norm.

Existence of unique solution for the field u. The regularization term $R(\mathbf{u})$ *guarantees* that there will always be a *unique* solution for the minimizer $\mathbf{u}$, i.e., the optimization problem of Eq. 25 can never be an under-determined problem, and there will be exactly one solution. See the discussion about the linear systems solution at the end of Sec. 5.3.

5.3 Matrix formulation and least-squares solution

We now formulate the minimization of the objective function given by Eq. 25 in matrix form to solve it in the least-squares (L_2) sense. We discretize the domain M into a grid of N sample points (ξ,τ). We use a regular grid that matches the grid where the input field $\mathbf{v}$ has been computed, and where $N=X\cdot Y\cdot Z\cdot T$, for a 3D field with T time steps.

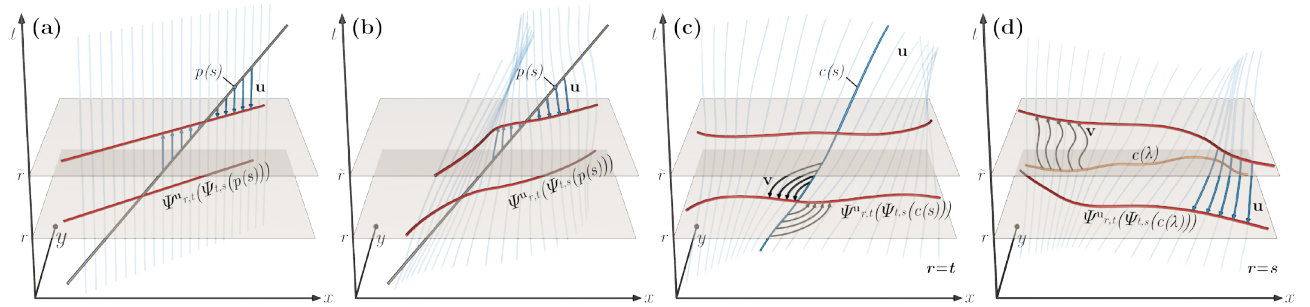

Fig. 5. **Visualization using observer velocity fields.** (a,b) Observed path lines (red). In (a), the observer field $\mathbf{u}(x,t) = 0$ (blue), i.e., all observers are stationary relative to $\mathbb{O}_0$. In this case, the observed path line is a standard path line, which is independent of the observation time r. In (b), the field $\mathbf{u}$ is an arbitrary observer field, where the path line visualization changes and depends on r. (c) Observed streak line. (d) Observed time line.

Velocity fields. We denote by $\mathbf{V}$ a vector of size $3N$ that contains the concatenation of all components of the input field $\mathbf{v}(x,t)$ for all (ξ,τ). Likewise, we denote by $\mathbf{U}$ a vector of size $3N$ that contains the velocity field $\mathbf{u}(x,t)$ for all (ξ,τ). However, $\mathbf{V}$ is a constant input vector, and the vector $\mathbf{U}$ contains the unknown variables that we are optimizing for.

Killing energy. We denote by $\mathbf{K}$ a matrix of size $9N \times 3N$ that contains the individual differential operators comprising the Killing operator K, to compute Eq. 24 for the entire field $\mathbf{u}$ as the product

$$\mathbf{E}_K = \mathbf{K} \cdot \mathbf{U}, \tag{29}$$

where the vector $\mathbf{E}_K$ (size $9N$) is the Killing operator evaluated on $\mathbf{u}$.

Observed time derivative. We denote by $\mathbf{D}$ a matrix of size $3N \times 3N$ that contains all differential operators comprising Eq. 16, as well as the pre-computed velocity gradient $\nabla\mathbf{v}$. All parts of Eq. 16 containing $\mathbf{u}$, i.e., everything except the term $\partial\mathbf{v}/\partial t$, are then obtained as the product

$$\mathbf{D}_t = \mathbf{D} \cdot \mathbf{U}. \tag{30}$$

Regularization. The linear part of the regularizer $\mathbf{v}_\mathbf{u} = \mathbf{v} - \mathbf{u} = 0$, which is $-\mathbf{u}$, can be evaluated via a diagonal matrix $\mathbf{N} = diag(-1)$ as

$$\mathbf{R} = \mathbf{N} \cdot \mathbf{U}. \tag{31}$$

Least-squares solution. For an over-determined linear system $\mathbf{Au} = \mathbf{b}$, i.e., where $\mathbf{A}$ is taller than wide, the least-squares (L_2) solution of the minimization problem $\min \frac{1}{2}||\mathbf{Au} - \mathbf{b}||_2^2$ can be computed as the solution of the normal equations [42] $\mathbf{A}^T\mathbf{A}\,\mathbf{u} = \mathbf{A}^T\mathbf{b}$, where $\mathbf{A}^T\mathbf{A}$ is square and positive (semi)definite. Therefore, we compute the minimizer of Eq. 25 as the least-squares solution to the system $\mathbf{A} \cdot \mathbf{U} = \mathbf{B}$, where the matrix $\mathbf{A}$, and the right-hand side vector $\mathbf{B}$, respectively, are given by

$$\mathbf{A} := \begin{bmatrix} \mathbf{K} \\ \lambda\,\mathbf{D} \\ \mu\,\mathbf{N} \end{bmatrix}, \qquad \mathbf{B} := -\begin{bmatrix} \mathbf{0} \\ \lambda\,\frac{\partial \mathbf{V}}{\partial t} \\ \mu\,\mathbf{V} \end{bmatrix}. \tag{32}$$

The matrix $\mathbf{A}$ has size $15N \times 3N$, the vector $\mathbf{B}$ size $15N$. The vector $\partial\mathbf{V}/\partial t$ contains the pre-computed time derivatives of the input field. The square system $\mathbf{A}^T\mathbf{A}$ to be solved is $3N \times 3N$, and $\mathbf{A}^T\mathbf{B}$ has size $3N$.

Existence of unique solution. Our optimization problem always has a unique solution due to the presence of the term $(\mu/2)\,||\mathbf{v}_\mathbf{u}||_2^2$, which acts as a Tikhonov regularizer [42]. The matrix $\mathbf{N}$ represents $3N$ linearly independent equations, and thus the matrix $\mathbf{A}$ ($15N$ linear equations) contains at least $3N$ linearly independent equations. Therefore, the rank of the $3N \times 3N$ system matrix $\mathbf{A}^T\mathbf{A}$ must be exactly $3N$.

6 Visualization using Observer Velocity Fields

Once an observer velocity field $\mathbf{u}(x,t)$ has been computed, we can employ two major perspectives for visualizing the input field $\mathbf{v}(x,t)$:

- Visualize $\mathbf{v}$ from the perspective of any individual observer $\mathbf{u}_i$.
- Visualize $\mathbf{v}$ from the *joint perspective* of all observers given by $\mathbf{u}$.

Below, we state everything with respect to the field $\mathbf{u}$, but for any individual observer $\mathbb{O}_i$ the same equations can be used after substituting $\mathbf{u}$ by $\mathbf{u}_i$, as given by Eq. 10. We will make extensive use of the concept of the flow of a time-dependent vector field, denoting the flow of the input field $\mathbf{v}$ by $\psi_{t,s}(x)$, and the flow of the observer field $\mathbf{u}$ by $\psi^\mathbf{u}_{t,s}(x)$.

6.1 The notion of *observation time*

Our goal now is to define a general framework for *visualizing* the input field $\mathbf{v}$ *relative to the observer field* $\mathbf{u}$, i.e., how the observers described by $\mathbf{u}$ perceive the field $\mathbf{v}$. A crucial observation is that, in general, this cannot be done without introducing the concept of a specific time with respect to which a visualization is computed. This is not required for standard visualization without an observer field, which can be seen as the special case $\mathbf{u} \equiv 0$. We call this special time the *observation time* r.

We can see this by considering the world lines $t \mapsto o_i(t)$ of some observers $\mathbb{O}_i$. These are integral curves of the field $\mathbf{u}$, which we can also think of as "curved time axes" for these observers. Figs. 5 (a) and (b) depict the same trajectory (gray) of a particle moving with constant velocity relative to $\mathbb{O}_0$, but two different observer fields $\mathbf{u}$ (blue). In Fig. 5 (a), all observer world lines are parallel to the time axis t, which is the world line of $\mathbb{O}_0$. The visualization of the particle's trajectory in space corresponds to orthogonal projection along the vertical $o_i(t)$ to the chosen time r. Here, the choice of r is irrelevant, because orthogonal projection always gives the same curve in space (red). In contrast, for a general field $\mathbf{u}$ (Killing or not Killing), a particle trajectory observed in space will curve differently. That is, as depicted in Fig. 5 (b), the *visualization* of the same trajectory (gray) depends, in general, on the choice of r. This fact is not restricted to a specific type of characteristic curve. It is equally true for stream lines, path lines, streak lines, and time lines. In the special case when $\mathbf{u}$ is Killing, visualizations of the same trajectory observed at different r will, in general, still be different. However, they will be the same up to isometries, corresponding to the *symmetry group* of Euclidean space [25]. We note, however, that if $\mathbf{u}$ rotates relative to $\mathbb{O}_0$, the red path lines in Fig. 5 (b) *will still be curved*.

Choosing an observation time. A specific choice of observation time for visualization can be interpreted as visualizing the field with this time as a "reference." However, all possible choices of reference are in general equally valid. This can be understood, for example, by considering a rigid rotation over time. Some time must be picked as the reference that corresponds to "no rotation," i.e., choosing a reference line with respect to which a relative angle is defined to be $0°$, or a rotation matrix is the identity. Although often there is no natural choice, *some* reference must be chosen, with respect to which relative measurements can be made. Similarly, our observed time derivatives can be integrated starting from some arbitrary choice of time r (see Eq. 38). But integration must start from some initial value, where here we would start with zero. But this is true for any arbitrary choice of r.

We can also think about the meaning of an observation time r as choosing a visualization of some characteristic curve *as it is observed by the observers described by* $\mathbf{u}$, *where they were at time* r. For a different time r, the same observers will *themselves* have moved. Therefore, their observation of the same characteristic curve will be different.

6.2 Observed characteristic curves

We now give precise definitions of *observed* versions of each of the major types of characteristic curves, starting with stream lines.

6.2.1 Observed stream lines

A standard stream line with a parameter λ instead of t, to avoid confusion with the actual time parameter t, for a time-dependent field $\mathbf{v}(x,t)$,

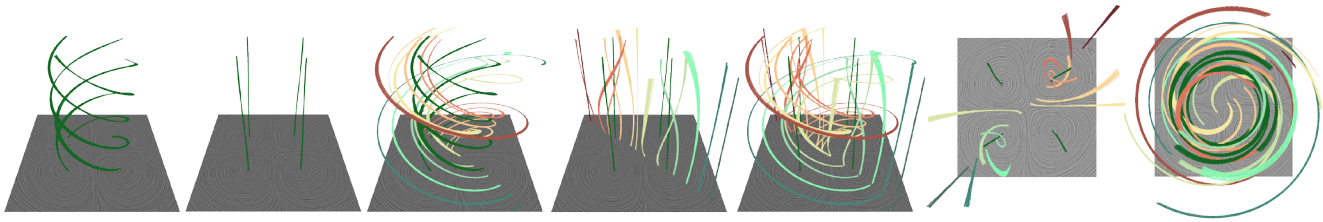

Fig. 6. **Visualization and objective vortex cores** (FOUR CENTERS flow). (a) Vortex cores are detected objectively, but visualized for the lab frame observer $\mathbb{O}_0$; LIC: $\mathbf{v}_\mathbf{u}$ for $r=t$. (b) The same cores, but as seen by the observer field $\mathbf{u}$ (using $\mathbf{w}_r$, see Sec. 6.3); LIC: $\mathbf{v}_\mathbf{u}$ for $r=0$ (see paper video). (c) Spatial relationships between path lines seeded close to vortex cores as well as farther away are unclear for $\mathbb{O}_0$. (d) The observer field $\mathbf{u}$ clearly sees which path lines are close to core lines and swirl around them, and which path lines are far away. The latter only look as though they are rotating in (c), because they rotate in the same way as the vortex cores do, as seen by $\mathbb{O}_0$. This fact is not visible in (c). In contrast, in (d) far-away path lines become stationary. (e) These observations can be confirmed by super-imposing (c) and (d). Image (f) is (d) seen top-down; (g) is (c) seen top-down.

at any fixed time t, through an arbitrary point $x \in M$, can be written as

$$\lambda \mapsto p(\lambda,t) := x + \int_0^\lambda \mathbf{v}\left(p(\gamma,t),t\right)\,\mathrm{d}\gamma, \quad \text{with } t,x \text{ fixed.} \tag{33}$$

Observed stream lines. We define an *observed stream line*, for the field $\mathbf{v}$ *observed relative to* the flow of the observer field $\mathbf{u}$, as

$$\lambda \mapsto p_\mathbf{u}(\lambda,t,r) := \psi^\mathbf{u}_{r,t}\left(x + \int_0^\lambda \mathbf{v}_\mathbf{u}\left(p_\mathbf{u}(\gamma,t,t),t\right)\,\mathrm{d}\gamma\right), \tag{34}$$

with t,x,r fixed, observed at a specific observation time r. (Note that $\psi^\mathbf{u}_{t,t}(x) = x$, and thus $p_\mathbf{u}(\gamma,t,t)$ gives a standard streamline of $\mathbf{v}_\mathbf{u}$.) The trivial choice is $r=t$, but r is arbitrary and stream lines can be mapped forward or backward in observation time. For example, if we want to *compare* different times t, we have to hold r constant and vary t. The paper video shows animated LIC sequences of observed stream lines for varying t but fixed $r=0$; Fig. 1 (left), Fig. 6 (b) show one time step.

We remark that our observed stream lines can be written as "advected stream lines" [49], when the field is $\mathbf{v}_\mathbf{u}$ and the "advection field" is $\mathbf{u}$.

6.2.2 Observed path lines

A standard path line through a point $x \in M$ at time s can be obtained from the flow $\psi_{t,s}(x)$ by varying the parameter t, holding s and x fixed:

$$t \mapsto p(t) := \psi_{t,s}(x) = x + \int_s^t \mathbf{v}\left(p(\tau),\tau\right)\,\mathrm{d}\tau, \quad \text{with } s,x \text{ fixed.} \tag{35}$$

Any flow must fulfill $\psi_{s,s}(x) = x$, and here we of course get $p(s) = x$.

Observed path lines. In order to obtain a path line as perceived by the field $\mathbf{u}$ at time r, we define an *observed path line* $t \mapsto p_\mathbf{u}(t,r)$ as

$$t \mapsto p_\mathbf{u}(t,r) := \psi^\mathbf{u}_{r,t}\Big(\psi_{t,s}\big(p(s)\big)\Big), \quad \text{with } s,r \text{ fixed.} \tag{36}$$

See Fig. 5 (a,b). A natural choice for the observation time might seem to be $r=s$, but this is arbitrary. In fact, there is no natural choice for s. Although we define a path line for a specific pair (x,s), any other $(\tilde{x},\tilde{s})$ identifies the same curve if it passes through x at time s, i.e., $\psi_{\tilde{s},s}(x) = \tilde{x}$ implies that $t \mapsto p(t) = \psi_{t,s}(x)$ is *equal* to $t \mapsto p(t) = \psi_{t,\tilde{s}}(\tilde{x})$. The same is true for the corresponding observed path line $t \mapsto p_\mathbf{u}(t,r)$. However, in general, the visualization will be different for different choices of r.

6.2.3 Observed path lines vs. observed stream lines

Standard path lines and stream lines. In the standard case, we can compare velocities at a fixed point x, at different times t and s, by

$$\mathbf{v}(x,t) = \mathbf{v}(x,s) + \int_s^t \frac{\partial \mathbf{v}(x,\tau)}{\partial \tau}\,\mathrm{d}\tau. \tag{37}$$

If the Eulerian time derivative term is zero, which is the same as saying that $\mathbf{v}$ is a steady field, path lines and stream lines will be identical.

Observed path lines and stream lines. Relative to an observer field $\mathbf{u}$, this becomes more complicated. The equivalent expression is

$$\mathbf{v}_\mathbf{u}\left(\psi^\mathbf{u}_{t,s}(x),t\right) = \mathrm{d}\psi^\mathbf{u}_{t,s}(x)\Big(\mathbf{v}_\mathbf{u}\left(x,s\right)\Big) + \int_s^t L_\mathbf{u}(\mathbf{v}_\mathbf{u})\left(\psi^\mathbf{u}_{\tau,s}(x),\tau\right)\mathrm{d}\tau. \tag{38}$$

That is, observed path lines and observed stream lines will be identical when the *observed time derivative*, i.e., the Lie derivative term, is zero. This is the case when $\mathbf{v}_\mathbf{u}$ is simply *pushed forward* by the flow $\psi^\mathbf{u}_{t,s}(x)$.

Since for our field $\mathbf{u}$ we minimize the Lie derivative $L_\mathbf{u}(\mathbf{v}_\mathbf{u})$ everywhere (Sec. 5), its integral will be as small as possible. *This makes all observed path lines as similar to stream lines as possible.* Referring ahead to Sec. 6.3, this also implies that our transformed observation time field $\mathbf{w}_r(x,t)$, for any choice of r, will also be as steady as possible.

6.2.4 Observed streak lines

A standard streak line through a seed point $x \in M$ can be obtained at time t from $\psi_{t,s}(x)$ by varying the parameter s, holding t and x fixed:

$$s \mapsto p(s) := \psi_{t,s}(x), \quad \text{with } t,x \text{ fixed.} \tag{39}$$

Here, we can interpret the parameter s by saying that, if the current time is t, then $s<t$ maps to particle positions that have been at x in the past, and $s>t$ maps to particle positions that will be at x in the future.

Dependence on choice of observer. Since streak lines are defined with respect to a *fixed* seeding position x, their construction inherently depends on the choice of observer with respect to which x is stationary. Thus, we want to allow the seeding position to move along an arbitrary curve $s \mapsto c(s)$ over time. This curve can be chosen such that, for some observer $\mathbb{O}_i$, it maps to the same point for all s, whereas for observers moving relative to $\mathbb{O}_i$, the seeding position moves with s. We define

$$s \mapsto p(s) := \psi_{t,s}\big(c(s)\big), \quad \text{with } t \text{ fixed.} \tag{40}$$

This type of streak line is equivalent to the *generalized streak lines* of Wiebel et al. [52], whose seeding position is also a curve over time.

Observed streak lines. Analogously to observed path lines, we can now define an *observed streak line* $s \mapsto p_\mathbf{u}(s,r)$, with r fixed, as

$$s \mapsto p_\mathbf{u}(s,r) := \psi^\mathbf{u}_{r,t}\Big(\psi_{t,s}\big(c(s)\big)\Big), \quad \text{with } t,r \text{ fixed.} \tag{41}$$

See Fig. 5 (c). The trivial choice for the observation time is $r=t$, but for comparing streak lines we again have to hold r constant while varying t. A natural choice for the seeding curve $c(s)$ is the world line of some observer $\mathbb{O}_i$, i.e., choosing $s \mapsto c(s) := o_i(s)$. Another obvious choice is the "vertical" world line of some point that is stationary for $\mathbb{O}_0$.

6.2.5 Observed time lines

A standard time line can be obtained, at some time t, as a curve parameterized by a parameter λ, with a seeding curve $\lambda \mapsto c(\lambda)$ *defined* for an arbitrary seeding time s, varying λ and holding t and s fixed:

$$\lambda \mapsto p(\lambda) := \psi_{t,s}\big(c(\lambda)\big), \quad \text{with } t,s \text{ fixed.} \tag{42}$$

In contrast to streak lines, time lines are defined with respect to a set of spatial positions at the *fixed time* s. Their construction is therefore independent of any observer, because all observers share the same absolute time, and all observers can agree on the spatial curve $c(\lambda)$.

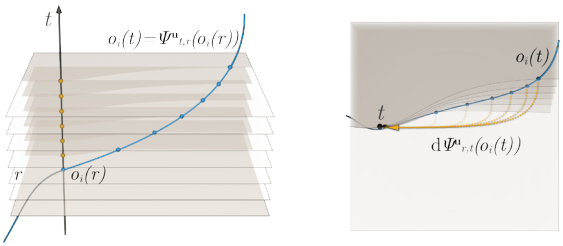

Fig. 7. **Observation time fields** allow computing any observed integral curve, for a specific observation time r, using standard integration. The "curved time axes" that are the world lines $o_i(t)$ of different observers, are each transformed to a straightened-out time axis, like the axis labeled t.

Observed time lines. Similar to the other observed integral curves, we can now define an *observed time line* $\lambda \mapsto p_{\mathbf{u}}(\lambda, r)$, with r fixed, as

$$\lambda \mapsto p_{\mathbf{u}}(\lambda, r) := \psi^{\mathbf{u}}_{r,t}\Big(\psi_{t,s}\big(c(\lambda)\big)\Big), \quad \text{with } t, s, r \text{ fixed.} \tag{43}$$

See Fig. 5 (d). Here, the indeed natural choice for the observation time is $r = s$, because the time line is *defined* for some fixed time s. In order to compare time lines, we simply hold $r = s$ constant while varying t.

6.3 Transformed observation time fields

Given the definition of an observed path line (Eq. 36), we can choose a fixed arbitrary observation time r, and directly compute the derivative of the observed path line $t \mapsto p_{\mathbf{u}}(t, r)$, with r fixed, for all times t.

For the path line $t \mapsto p(t) := \psi_{t,s}(x)$, through $x = p(s) \in M$ at time s, the derivative of the corresponding observed path line at any $t = \tau$ is

$$\left.\frac{\mathrm{d}}{\mathrm{d}t}\right|_{t=\tau} t \mapsto p_{\mathbf{u}}(t, r) = \mathrm{d}\psi^{\mathbf{u}}_{r,\tau}(p_\tau)\Big(\mathbf{v}_{\mathbf{u}}(p_\tau, \tau)\Big), \tag{44}$$

where we define $p_\tau := \psi_{\tau,s}(p(s)) \in M$. The linear map $\mathrm{d}\psi^{\mathbf{u}}_{r,\tau}(p_\tau)$ is the differential (the push-forward) of the map $\psi^{\mathbf{u}}_{r,\tau}(x)$, evaluated at $x = p_\tau$. See App. E (suppl. material) for the detailed derivation of Eq. 44.

Observation time fields. For any fixed r, we can now *define* a field $(x, t) \mapsto \mathbf{w}_r(x, t)$, the *observation time field* for observation time r, by

$$\mathbf{w}_r(x, t) := \mathrm{d}\psi^{\mathbf{u}}_{r,t}(p_r(x, t))\Big(\mathbf{v}_{\mathbf{u}}(p_r(x, t), t)\Big), \tag{45}$$

where $p_r(x, t) := \psi^{\mathbf{u}}_{t,r}(x)$. Considering observer world lines $o_i(t)$, this means choosing $t_0 = r$, and tracking the observers with world lines $o_i(t) := \psi^{\mathbf{u}}_{t,t_0}(o_i(t_0))$. See Fig. 7. From $\mathbf{w}_r(x, t)$, we can compute any observed path line, through any point $p_{\mathbf{u}}(s, r)$, via standard integration,

$$t \mapsto p_{\mathbf{u}}(t, r) = p_{\mathbf{u}}(s, r) + \int_s^t \mathbf{w}_r\big(p_{\mathbf{u}}(\tau, r), \tau\big)\, \mathrm{d}\tau, \quad \text{with } s, r \text{ fixed.} \tag{46}$$

In fact, this approach is not restricted to path lines. The same $\mathbf{w}_r(x, t)$ can be used directly to compute *any observed integral curve* of $\mathbf{v}$, observed by $\mathbf{u}$ at time r, using the corresponding standard integration.

The *meaning* of an observation time field $\mathbf{w}_r$ is that it *is* the input vector field $\mathbf{v}$, *as it is perceived by the observers* described by $\mathbf{u}$, with respect to where these observers were at the chosen observation time r. This is, in general, the best we can conceptually do to *transform* the input field to what another observer or a whole observer field perceives.

We note that while Eq. 45 is defined for a general $\mathbf{u}$, it is straightforward to simplify for special cases. If $\mathbf{u}$ describes, e.g., rigid motion, both $\psi^{\mathbf{u}}_{t,r}(x)$ and $\mathrm{d}\psi^{\mathbf{u}}_{r,t}(x)$ need essentially only be computed for one x.

For any other observation time $\tilde{r}$, we simply compute $\mathbf{w}_{\tilde{r}}(x, t)$. We can of course also pre-compute the fields $\mathbf{w}_r(x, t)$ for all possible r. This collection of vector fields can be seen as one vector field over a domain of one dimension higher, i.e., we can consider a single field $\mathbf{w}(x, t, r)$. We note that this is similar in spirit to streak line vector fields [51].

7 Observer Velocity Fields and Frame Indifference

In order for the observer velocity field to be indifferent to the frame of reference in which it was computed, i.e., the observer $\mathbb{O}_0$, it must (1) be obtained as the unique solution of the corresponding optimization problem. This is guaranteed by our regularization, as discussed above (Sec. 5). (2) We also have to show that the optimization will find *the same* minimum for any arbitrary choice of observer $\mathbb{O}_0$, $\bar{\mathbb{O}}_0$, ... We therefore have to consider each term in the objective function Eq. 25.

In the term E_K we have, in fact, twice the rate-of-strain (rate-of-deformation) tensor from continuum mechanics, which is known to be an objective second-order tensor [17]. Any such tensor $\mathbf{W}$ transforms [46] according to $\bar{\mathbf{W}} = \mathbf{Q}(t)\,\mathbf{W}\,\mathbf{Q}(t)^T$, where $\mathbf{Q}(t)$ is a time-dependent orthogonal transformation. We thus obtain the same minimum for this term independent of observer, since with $\mathbf{Q}(t)$ orthogonal,

$$\|K\bar{\mathbf{u}}\|_F = \big\|\mathbf{Q}(t)\,(K\mathbf{u})\,\mathbf{Q}(t)^T\big\|_F = \|K\mathbf{u}\|_F\,. \tag{47}$$

For the term D_t, we know that the Lie derivative of an objective tensor is objective, even though the vector field $\mathbf{u}$ is not [32, Th. 6.19]. Therefore, since the relative velocity $\mathbf{v}_{\mathbf{u}}$ is an objective vector (see App. F, suppl. material), the expression $L_{\mathbf{u}}(\mathbf{v}_{\mathbf{u}})$ is also an objective vector. Any objective vector $\mathbf{w}$ transforms [46] according to $\bar{\mathbf{w}} = \mathbf{Q}(t)\,\mathbf{w}$. Thus,

$$\|L_{\bar{\mathbf{u}}}(\bar{\mathbf{v}}_{\bar{\mathbf{u}}})\|_2 = \|\mathbf{Q}(t)\,(L_{\mathbf{u}}(\mathbf{v}_{\mathbf{u}}))\|_2 = \|L_{\mathbf{u}}(\mathbf{v}_{\mathbf{u}})\|_2\,. \tag{48}$$

For the term R, we again use that $\mathbf{v}_{\mathbf{u}}$ is objective, and thus, likewise,

$$\|\bar{\mathbf{v}}_{\bar{\mathbf{u}}}\|_2 = \|\mathbf{Q}(t)\,(\mathbf{v}_{\mathbf{u}})\|_2 = \|\mathbf{v}_{\mathbf{u}}\|_2\,. \tag{49}$$

Therefore, since each term is invariant with respect to observer transformations, optimization with the objective function Eq. 25 is invariant as well. This makes features such as vortices, computed using standard approaches that by themselves are non-objective, indifferent to the observer $\mathbb{O}_0$ for whom the input flow was given, and thus objective.

Table 1. ***Data sets and computation times*** for optimization of $\mathbf{u}$, and computation of an observation time field $\mathbf{w}_r$ for one observation time r.

Data set	Grid resolu.	Time steps	$\mathbf{u}(x,t)$	$\mathbf{w}_r(x,t)$
Four Centers	64×64	64	2:15 min	47 sec
2D Vortex Street	400×50	1001	2:24 hrs	1:00 hrs
3D Vortex Street	$192 \times 64 \times 48$	102	7:12 hrs	-
Ocean	390×210	14	3 min	67 sec

8 Results

We illustrate observer field-relative visualization and objective vortex detection using standard vortex measures. We have implemented the optimization as well as the computation of $\mathbf{w}_r$ in MATLAB, solving the sparse linear system from Sec. 5.3 with a pre-conditioned incomplete Cholesky conjugate gradient solver. See Table 1 for an overview. Our approach only requires first-order derivatives, which we compute via finite differences on a regular grid. We also estimate flow differentials via central differences, which is common in FTLE computations [40].

Vortex cores. Observation time fields are objective and *as steady as possible*. Thus, objective vortex cores can be computed in each $\mathbf{w}_r$ with standard methods for *steady* flow. In 2D, we track vortex core lines in a feature flow field [45], starting at the critical points of $\mathbf{w}_r$ where $\nabla\mathbf{w}_r$ has complex eigenvalues. In 3D, the Sujudi-Haimes criterion [44] or parallel vectors operator [36] can be used in $\mathbf{w}_r$. Vortices can also be computed directly from $\mathbf{v}_{\mathbf{u}}$ and objective derivatives (Secs. 4.3 and 4.4).

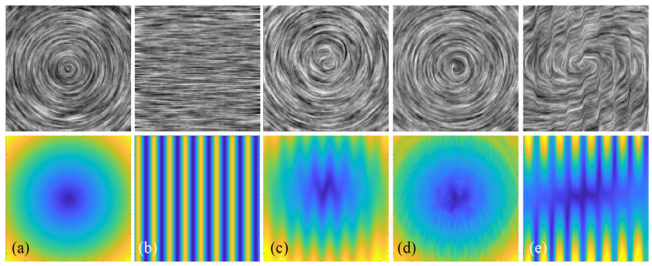

Fig. 8. **Comparison with *generic objective vortices* [17].** Observing an original field that is a steady rigid body rotation (a) from an observer field with a horizontal wave-form modulation of velocity magnitude (b), gives a new unsteady input field (c). Our method can reconstruct a good approximation of the original field (d). The fixed neighborhood of [17] prevents proper reconstruction (e). Top: LIC; Bottom: velocity magnitude.

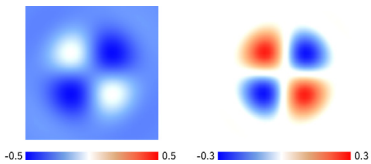

Fig. 9. **Vorticity comparison.** We compare the vorticity of the FOUR CENTERS flow. (Left) Regular vorticity of the input flow $\mathbf{v}$. (Right) Observed flow $\mathbf{v}_\mathbf{u}$ with *objective vorticity*, computed from a corresponding $\mathbf{w}_r$.

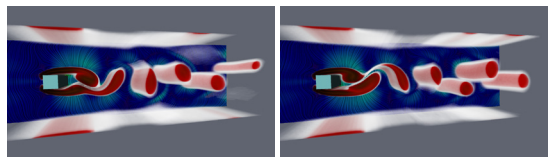

Fig. 10. **Objective vorticity** in two selected time steps of the observed field $\mathbf{v}_\mathbf{u}$ of the 3D VORTEX STREET flow. Volume renderings of objective vorticity magnitude, computed using $\mathbf{u}$ and Eq. 19, highlight vortices.

Rotating four centers with objective core lines. We compute the vortex core lines of the FOUR CENTERS flow used in previous work [17, 18]. The observer $\mathbb{O}_0$ undergoes a time-dependent rotation relative to an originally steady flow field, which makes our input field $\mathbf{v}$ unsteady. The equation for the unsteady input field $\mathbf{v}$ is given in the supp. material. Fig. 6 illustrates the objective detection of the four vortex core lines from the unsteady input field $\mathbf{v}$. Fig. 9 compares the vorticity of the lab frame input flow with the objective vorticity seen by the observer field.

Observer-relative visualization of core lines and swirling particles. Fig. 6 shows that the observation time field $\mathbf{w}_r$ enables visualizing the input flow $\mathbf{v}$ *objectively* as perceived by the observer field $\mathbf{u}$. We note that it is hardly possible to discern spatial relationships between path lines and the core lines when the field is visualized from the perspective of the lab frame observer $\mathbb{O}_0$, even though all vortex core lines were tracked objectively. In contrast, the visualizations computed from the observation time field $\mathbf{w}_r$ show clean, vertical core lines in space-time, and the swirling motion of particles is clearly visible.

2D time-dependent vortex street. Fig. 1 shows a 2D VORTEX STREET, which is a 2D flow field containing a von Kármán vortex street that develops behind a circular cylinder. It has been simulated by Tino Weinkauf [51] using the Free Software *Gerris Flow Solver* [38]. Fig. 1 (left) uses a field $\mathbf{u}$ computed with $\lambda = 1.0, \mu = 0.05$. Fig. 4 illustrates zoom-ins for this flow field with four different observer fields computed with different optimization parameters λ, μ. Fig. 11 (in the supplementary material) illustrates more parameter combinations.

3D time-dependent vortex street. Fig. 10 shows volume-rendered vortices computed from *objective* vorticity magnitude for a 3D time-dependent flow. Vorticity has been computed from our optimized $\mathbf{u}$ via Eq. 19. This 3D VORTEX STREET flow field [12, 24, 48] contains a von Kármán vortex street that develops behind a square cylinder. See App. I (suppl. material) for detailed data set acknowledgments.

9 DISCUSSION

Performance. The timings reported in Table 1 are from our current proof-of-concept MATLAB implementation. The optimization itself can certainly be optimized further. However, a current intrinsic limitation is that we globally optimize over all time steps, and computation time goes up with longer time sequences. In contrast, the time for computing observation time fields $\mathbf{w}_r$ could trivially be made orders of magnitude faster by a parallel C++/OpenMP or GPU implementation.

General observer fields vs. approximate Killing fields. The approximate Killing property of the observer field $\mathbf{u}$ is often desirable, because it gives visualizations with as little deformation as possible, and it makes nearby observers "as similar as possible." However, the major methods presented in this paper do not depend on $\mathbf{u}$ being approximately Killing. They are, in fact, very general and work for any general field $\mathbf{u}$. In particular, observed time derivatives (Sec. 4.3) as well as observer field-relative visualization (Sec. 6) work for any $\mathbf{u}$.

Comparison with *generic objective vortices* [17]. A major benefit of our framework is that it works globally, but implicitly still adapts locally. In contrast, the approach of Günther et al. [17] depends on a fixed neighborhood size that is not adapted to local features of possibly different size. Fig. 8 shows a simple example where this makes a big difference. We observe an originally static rigid body rotation from an observer field that has a velocity magnitude profile modulated by a horizontal wave function. This gives an unsteady input field $\mathbf{v}$, from which we reconstruct the original steady field. Fig. 8 (d) shows the reconstruction of the original rotating field using our method. Fig. 8 (e) shows the reconstruction using the public code provided for the method of Günther et al. [17] using the default neighborhood size setting of 10.

10 CONCLUSIONS

We have presented the first general framework for modeling a continuous, smooth field of observers for unsteady flow visualization and objective feature detection, such as objectively detecting vortices in unsteady flow fields. We compute the observer field such that it globally minimizes the *observed time derivative*, as perceived by the observer field. This makes the observed field *as steady as possible*. We see the biggest contribution of our method in the rigorous definition of the differential quantities that should be minimized in such an approach, and that we employ a single global optimization over space and time for computing the observer field such that these differential properties are globally minimized. Because of this, we do not have to specify a neighborhood size for computation, while at the same time we are not restricted to modeling a single global observer motion. We see the restriction to either a single global observer or a separate local observer per point as the biggest drawbacks of prior work targeting objectivity.

Furthermore, we believe that it is important to have a general framework available that allows visualizing directly *what the modeled observers actually perceive*, e.g., Fig. 1 (left) and Fig. 6 (b,d,f). Even previous objective approaches usually visualize features, such as vortex core lines, relative to the lab frame observer $\mathbb{O}_0$ for which the input was given. However, the fact that for unsteady flow one tries to *compute* features relative to other observers shows that it is important to also be able to *visualize* relative to these observers. We have shown that this goes further than computing objective vortex core lines, but enables the visualization of core lines as well as the path lines swirling around them as "stationary" curves parallel to the perceived time axis in space-time.

ACKNOWLEDGMENTS

We thank Anna Frühstück for the illustrations and for help with the figures and the video, Holger Theisel for helpful discussions, and the anonymous reviewers for helpful comments. This work was supported by King Abdullah University of Science and Technology (KAUST). This research used resources of the Core Labs of King Abdullah University of Science and Technology (KAUST). See App. I (supplementary material) for data set acknowledgments.

A THE LIE DERIVATIVE

The *Lie derivative* measures the differential change of a tensor field on a manifold M, with respect to the flow generated by a vector field on M. For a time-independent tensor field $\mathbf{t}$ on M, the Lie derivative $\mathscr{L}$ with respect to a vector field $\mathbf{u}$ with flow ϕ_t, is defined, at a point $x \in M$, as

$$\left(\mathscr{L}_\mathbf{u}\,\mathbf{t}\right)_x := \left.\frac{\mathrm{d}}{\mathrm{d}t}\right|_{t=0} \mathrm{d}\phi_{-t}\left(\mathbf{t}_{\phi_t(x)}\right), \tag{50}$$

where $\mathrm{d}\phi_t$ is the differential of the flow ϕ_t, and $\phi_{-t} = \phi_t^{-1}$. When $\mathbf{t}$ is a vector field $\mathbf{v}$, the Lie derivative $\mathscr{L}_\mathbf{u}\mathbf{v}$ is the same as the Lie bracket [16, Ch. 4] between the two vector fields, i.e., $\mathscr{L}_\mathbf{u}\mathbf{v} = [\mathbf{u}, \mathbf{v}]$. The Lie bracket, and thus for this case the Lie derivative, can be expanded as [32, p.103]

$$\mathscr{L}_\mathbf{u}\,\mathbf{v} = \nabla\mathbf{v}\,(\mathbf{u}) - \nabla\mathbf{u}\,(\mathbf{v}). \tag{51}$$

If the field $\mathbf{t}$ is time-dependent, the definition of the Lie derivative must be extended to the time-dependent Lie derivative [32, p.95], which is

$$\left(L_\mathbf{u}\,\mathbf{t}\right)_x := \left.\frac{\mathrm{d}}{\mathrm{d}t}\right|_{t=s} \mathrm{d}\psi_{s,t}\left(\mathbf{t}_{\psi_{t,s}(x)}\right) = \left(\frac{\partial\mathbf{t}}{\partial t} + \mathscr{L}_\mathbf{u}\,\mathbf{t}\right)_x, \tag{52}$$

at a point $x \in M$, at time s. For a time-dependent vector field $\mathbf{v}$, this is

$$L_\mathbf{u}\,\mathbf{v} = \frac{\partial\mathbf{v}}{\partial t} + \mathscr{L}_\mathbf{u}\mathbf{v}. \tag{53}$$

We refer to Marsden and Hughes [32, Ch. 1.6], and Frankel [16, Ch. 4].

REFERENCES

[1] M. Alexa, D. Cohen-Or, and D. Levin. As-rigid-as-possible shape interpolation. In *Proceedings of SIGGRAPH 2000*, pp. 157–164, 2000.

[2] V. I. Arnold. *Mathematical Methods of Classical Mechanics*. Springer-Verlag, 2nd ed., 1989.

[3] O. Azencot, M. Ben-Chen, F. Chazal, and M. Ovsjanikov. An operator approach to tangent vector field processing. *Computer Graphics Forum*, 32(5):73–82, 2013.

[4] O. Azencot, M. Ovsjanikov, F. Chazal, and M. Ben-Chen. Discrete derivatives of vector fields on surfaces–an operator approach. *ACM Transactions on Graphics*, 34(3):Article No. 29, 2015.

[5] G. K. Batchelor. *An Introduction to Fluid Dynamics*. Cambridge University Press, 2000.

[6] M. Ben-Chen, A. Butscher, J. Solomon, and L. Guibas. On discrete Killing vector fields and patterns on surfaces. In *Proceedings of Eurographics Symposium on Geometry Processing*, pp. 1701–1711, 2010.

[7] H. Bhatia, G. Norgard, V. Pascucci, and P.-T. Bremer. The Helmholtz-Hodge decomposition–a survey. *IEEE Transactions on Visualization and Computer Graphics*, 19(8):1386–1404, 2013.

[8] H. Bhatia, V. Pascucci, and P.-T. Bremer. The natural Helmholtz-Hodge decomposition for open-boundary flow analysis. *IEEE Transactions on Visualization and Computer Graphics*, 20(11):1566–1578, 2014.

[9] H. Bhatia, V. Pascucci, R. M. Kirby, and P.-T. Bremer. Extracting features from time-dependent vector fields using internal reference frames. *Computer Graphics Forum*, 33(3):21–30, 2014.

[10] R. Bujack, M. Hlawitschka, and K. I. Joy. Topology-inspired Galilean invariant vector field analysis. In *Proceedings of IEEE Pacific Visualization 2016*, pp. 72–79, 2016.

[11] B. Cabral and L. C. Leedom. Imaging vector fields using line integral convolution. In *Proceedings of SIGGRAPH '93*, pp. 263–270, 1993.

[12] S. Camarri, M.-V. Salvetti, M. Buffoni, and A. Iollo. Simulation of the three-dimensional flow around a square cylinder between parallel walls at moderate Reynolds numbers. In *XVII Congresso di Meccanica Teorica ed Applicata*, 2005.

[13] K. Y. K. Chan and J. W. L. Wan. Reconstruction of missing cells by a Killing energy minimizing nonrigid image registration. In *Conference of the IEEE Engineering in Medicine and Biology Society (EMBC)*, pp. 3000–3003, 2013.

[14] F. de Goes, B. Liu, M. Budninskiy, Y. Tong, and M. Desbrun. Discrete 2-tensor fields on triangulations. *Computer Graphics Forum*, 33(5):13–24, 2014.

[15] M. P. do Carmo. *Riemannian Geometry*. Birkhäuser, 1992.

[16] T. Frankel. *The Geometry of Physics: An Introduction*. Cambridge University Press, 3rd ed., 2011.

[17] T. Günther, M. Gross, and H. Theisel. Generic objective vortices for flow visualization. *ACM Transactions on Graphics*, 36(4):Article No. 141, 2017.

[18] T. Günther, M. Schulze, and H. Theisel. Rotation invariant vortices for flow visualization. *IEEE Transactions on Visualization and Computer Graphics*, 22(1):817–826, 2016.

[19] T. Günther and H. Theisel. The State of the Art in Vortex Extraction. *Computer Graphics Forum*, 37(6):149–173, Sept. 2018.

[20] G. Haller. An objective definition of a vortex. *Journal of Fluid Mechanics*, 525:1–26, 2005.

[21] G. Haller, A. Hadjighasem, M. Farazmand, and F. Huhn. Defining coherent vortices objectively from the vorticity. *Journal of Fluid Mechanics*, 795:136–173, 2016.

[22] G. A. Holzapfel. *Nonlinear Solid Mechanics: A Continuum Approach for Engineering*. Wiley, 2000.

[23] T. Igarashi, T. Moscovich, and J. F. Hughes. As-rigid-as-possible shape manipulation. *ACM Transactions on Graphics*, 24(3):1134–1141, 2005.

[24] International CFD Database, http://cfd.cineca.it/.

[25] N. Jeevanjee. *An Introduction to Tensors and Group Theory for Physicists*. Birkhäuser Boston, 2nd ed., 2015.

[26] J. Jeong and F. Hussain. On the identification of a vortex. *Journal of Fluid Mechanics*, 285:69–94, 1995.

[27] B. Jobard, G. Erlebacher, and M. Y. Hussaini. Lagrangian-Eulerian advection of noise and dye textures for unsteady flow visualization. *IEEE Transactions on Visualization and Computer Graphics*, 8(3):211–222, 2002.

[28] M. Kilian, N. J. Mitra, and H. Pottmann. Geometric modeling in shape space. *ACM Transactions on Graphics*, 26(3):Article No. 64, 2007.

[29] J. M. Lee. *Introduction to Smooth Manifolds*. Springer-Verlag, 2nd ed., 2012.

[30] G.-S. Li, X. Tricoche, and C. Hansen. GPUFLIC: Interactive and accurate dense visualization of unsteady flows. In *Proceedings of Eurovis 2006*, pp. 29–34, 2006.

[31] H. J. Lugt. The dilemma of defining a vortex. In *Recent Developments in Theoretical and Experimental Fluid Mechanics: Compressible and Incompressible Flows*, pp. 309–321. Springer-Verlag, 1979.

[32] J. E. Marsden and T. J. Hughes. *Mathematical Foundations of Elasticity*. Dover Publications, Inc., 1994.

[33] J. Martinez Esturo, C. Rössl, and H. Theisel. Generalized metric energies for continuous shape deformation. In *Mathematical Methods for Curves and Surfaces*, Lecture Notes in Computer Science, pp. 135–157. Springer-Verlag, 2012.

[34] A. McInerney. *First Steps in Differential Geometry*. Springer-Verlag, 2013.

[35] R. W. Ogden. *Non-Linear Elastic Deformations*. Dover Publications, Inc., 1997.

[36] R. Peikert and M. Roth. The "Parallel Vectors" operator–a vector field visualization primitive. In *Proceedings of IEEE Visualization '99*, pp. 263–532, 1999.

[37] P. Petersen. *Riemannian Geometry*. Springer-Verlag, 3rd ed., 2016.

[38] S. Popinet. Free computational fluid dynamics. *ClusterWorld*, 2(6), 2004.

[39] P. G. Saffman. *Vortex Dynamics*. Cambridge University Press, 1995.

[40] S. C. Shadden. *A dynamical systems approach to unsteady systems*. PhD thesis, California Institute of Technology, Pasadena, CA, 2006.

[41] H.-W. Shen and D. L. Kao. UFLIC: A line integral convolution algorithm for visualizing unsteady flows. In *Proceedings of IEEE Visualization '97*, pp. 317–322, 1997.

[42] J. Solomon. *Numerical Algorithms*. AK Peters/CRC Press, 2015.

[43] J. Solomon, M. Ben-Chen, A. Butscher, and L. Guibas. As-Killing-as-possible vector fields for planar deformation. In *Proceedings of Eurographics Symposium on Geometry Processing*, pp. 1543–1552, 2011.

[44] D. Sujudi and R. Haimes. Identification of swirling flow in 3-d vector fields. In *Proceedings of the 12th Computational Fluid Dynamics Conference*, pp. 792–799, 1995.

[45] H. Theisel and H.-P. Seidel. Feature flow fields. In *Proceedings of the Symposium on Data Visualisation 2003*, pp. 141–148, 2003.

[46] C. Truesdell and W. Noll. *The Nonlinear Field Theories of Mechanics*. Springer-Verlag, 1965.

[47] J. J. van Wijk. Image based flow visualization. *ACM Transactions on Graphics*, 21(3):745–754, 2002.

[48] W. von Funck, T. Weinkauf, H. Theisel, and H.-P. Seidel. Smoke surfaces: An interactive flow visualization technique inspired by real-world flow experiments. *IEEE Transactions on Visualization and Computer Graphics*, 14(6):1396–1403, 2008.

[49] T. Weinkauf, H.-C. Hege, and H. Theisel. Advected tangent curves: A general scheme for characteristic curves of flow fields. *Computer Graphics Forum*, 31(2):825–834, 2012.

[50] T. Weinkauf, J. Sahner, H. Theisel, and H.-C. Hege. Cores of swirling particle motion in unsteady flows. *IEEE Transactions on Visualization and Computer Graphics*, 13(6):1759–1766, 2007.

[51] T. Weinkauf and H. Theisel. Streak lines as tangent curves of a derived vector field. *IEEE Transactions on Visualization and Computer Graphics*, 16(6):1225–1234, 2010.

[52] A. Wiebel, X. Tricoche, D. Schneider, H. Jänicke, and G. Scheuermann. Generalized streak lines: Analysis and visualization of boundary induced vortices. *IEEE Transactions on Visualization and Computer Graphics*, 13(6):1735–1742, 2007.